Struct Multidisc Optim (2009) 39:1–15
DOI 10.1007/s00158-008-0333-5

RESEARCH PAPER

Topological sensitivity derivative and finite topology modifications: application to optimization of plates in bending

Dariusz Bojczuk · Zenon Mróz

Received: 21 June 2008 / Revised: 1 October 2008 / Accepted: 19 October 2008 / Published online: 21 November 2008

Abstract The concept of topological sensitivity derivative is introduced and applied to study the problem of optimal design of structures. It is assumed, that virtual topology variation is described by topological parameters. The topological derivative provides the gradients of objective functional and constraints with respect to these parameters. This derivative enables formulation of the conditions of topology transformation. In this paper formulas for the topological sensitivity derivative for bending plates are derived. Next, the topological derivative is used in the optimization process in order to formulate conditions of finite topology modifications and in order to localize positions of the modifications. In the case of plates they are related to introduction of holes and introduction of stiffeners. The theoretical considerations are illustrated by some numerical examples.

Keywords Topological sensitivity derivative · Finite topology modifications · Bending plates · Optimal topology and shape · Optimal layout of ribs

D. Bojczuk (✉)
Faculty of Management and Computer Modelling, Kielce University of Technology, Kielce, Poland
e-mail: mecdb@eden.tu.kielce.pl

Z. Mróz
Institute of Fundamental Technological Research, Warsaw, Poland
e-mail: zmroz@ippt.gov.pl

1 Introduction

The problems of optimal design with account for topology modification have been recently studied both for material and structural parameters. In the case of material parameters the topology variation corresponds to introduction of voids, inclusions, cracks, nucleation of different crystalline phases, etc. When structural parameters are used the topology variation corresponds to introduction or removing of holes, stiffeners, members, supports, nodes etc., and to replacement of existing elements by new elements.

The uniform treatment of topology and shape optimization by modification of material can be obtained by assuming a microstructure with its parameters optimized at the element level, for instance, by homogenization technique and with the spatial evolution of microstructure generated by a global solution for the whole structure. A simplified approach of this type is based on the artificial density distribution specifying the microstructure evolution in terms of one scalar variable, cf. Bendsoe and Kikuchi (1988), Bendsoe (1997) and Allaire (2002). The stiffness moduli are assumed to be proportional to the relative material density raised to some power. A number of numerical schemes have been developed within the homogenization method using the penalization of intermediate densities (SIMP-method). An alternative approach such as bubble method proposed by Eschenauer et al. (1994), generates the topology variation by introduction of holes into the structure domain with subsequent optimization of their position, size and shape. An alternative variant of this method was presented by Xie and Steven (1993), where the concept of gradual removal of the material in order to attain the optimal design is used.

This approach based on evolutionary strategy (ESO) proved to be efficient in effective redesign of structural elements. The concept of virtual topology variation and topological sensitivity derivative for truss and beam structures by specifying a class of admissible topologies in the redesign process was introduced by Bojczuk and Mróz (1998a, b, 1999, 2005) and Mróz and Bojczuk (2000). The topological sensitivity derivative provides the gradients of objective function and constraints with respect to topology parameters. This derivative provides the conditions for acceptance or rejection of a new topology. Once a new topological structure is accepted, the usual shape and material optimization is performed in order to determine optimal configuration, cross-sectional and material parameters. The case of hole generation in an elastic material was studied by Sokołowski and Żochowski (1999), Cea et al. (2000), Garreau et al. (2001), Novotny et al. (2005), Bojczuk and Szteleblak (2006), Mróz and Bojczuk (2006), while the case of reinforcement introduction was examined by Bojczuk (2006), Mróz and Bojczuk (2006), Bojczuk and Szteleblak (2008), where analytical expressions for the topological sensitivity derivative were derived and applied. The evolutionary algorithms combined with the boundary element method were developed by Burczyński and Kokot (2003) and applied in topology and shape optimization. The optimality conditions for simultaneous topology and shape optimization under volume constraints were formulated by Sokolowski and Żochowski (2003). The review of optimal topology design of truss or plate structures was provided by Kirsch (1989).

The combined shape and topology optimization was recently developed by applying the level-set-based method originally devised by Osher and Sethian (1988). This approach was used in the papers by Sethian and Wiegmann (2000), Osher and Santosa (2001), Allaire et al. (2002, 2004), Wang et al. (2004) and Xia et al. (2006). Relationship between the level set method and the topological derivative was analyzed in the pioneering papers by Burger et al. (2004) and Allaire et al. (2005). In fact, the shape sensitivity for an assumed integral of state fields is expressed in terms of boundary energy or mutual energy of primary and adjoint states, cf. Dems and Mróz (1984) or Petryk and Mróz (1996). The optimality conditions then require uniform values of generalized energy on the varying boundary. In the level-set method, the structure boundary is assumed to coincide with the iso-values of the assumed scalar function Φ representing the generalized energy with higher values within the structure domain and lower in its exterior. The generation of holes is then naturally induced in domains of lower values of Φ than the assumed design value.

In Section 2 the formulas for topological derivative with respect to introduction of circular holes into plates are derived. In Section 3 the topological derivative with respect to introduction of ribs is discussed. Some heuristic algorithms of optimization of plates based on topological derivatives are presented in Section 4. In Section 5 problems of topology, shape and reinforcement optimization of plate structures are discussed and illustrated by simple examples.

2 Topological derivative with respect to introduction of hole into a plate in bending

Consider now a plate in bending, whose middle surface occupies the domain $A \subset R^2$, with a boundary Γ. The plate is subjected to transverse load $\mathbf{p}^0$ in A, whereas either generalized traction $\mathbf{T}^0$ or displacements $\mathbf{u}^0$ are specified on Γ. Here, the Kirchhoff theory of thin plates is applied.

The topological derivative of functional G with respect to introduction of infinitesimally small circular hole (Fig. 1), analogously as in Sokołowski and Żochowski (1999), is defined as follows

$$T^G_{,A_0}(\mathbf{x}) = \lim_{\rho \to 0} \frac{G(A_\rho) - G(A)}{\pi \rho^2}, \quad \mathbf{x} \in A, \tag{1}$$

where $A_\rho = A - \bar{B}_\rho(\mathbf{x})$ and $\bar{B}_\rho(\mathbf{x})$ denotes a circular hole of area A_0 with its center at the point $\mathbf{x}$ and radius ρ, so $\bar{B}_\rho(\mathbf{x}) = \{\mathbf{y} \in R^2 : |\mathbf{y} - \mathbf{x}| \leq \rho\}$. Let us notice, that this formulation of the topological derivative is valid only in the case, when Neuman or free boundary conditions are satisfied on the hole boundary.

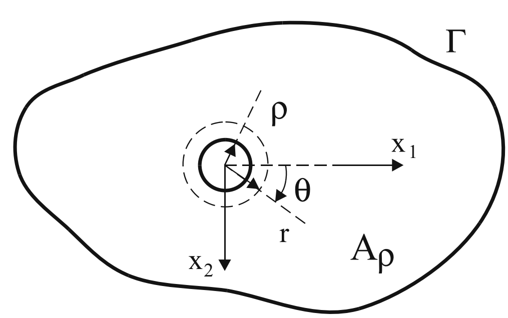

Fig. 1 Introduction of circular hole of radius ρ

2.1 Basic relations for plates in the polar coordinates

The stress–strain law, in the polar coordinates r, θ takes the form

$$M_{rr} = D\left(\kappa_{rr} + \nu\kappa_{\theta\theta}\right),$$
$$M_{\theta\theta} = D\left(\kappa_{\theta\theta} + \nu\kappa_{rr}\right),$$
$$M_{r\theta} = \frac{1}{2}\left(1-\nu\right) D\kappa_{r\theta}, \tag{2}$$

where M_{rr}, $M_{\theta\theta}$, $M_{r\theta}$ are the bending moments, $D = \frac{Eh^3}{12(1-\nu^2)}$ denotes the stiffness modulus of the plate and ν is the Poisson ratio. The curvatures are

$$\kappa_{rr} = -\frac{\partial^2 w}{\partial r^2},$$
$$\kappa_{\theta\theta} = -\frac{1}{r}\frac{\partial w}{\partial r} - \frac{1}{r^2}\frac{\partial^2 w}{\partial \theta^2},$$
$$\kappa_{r\theta} = 2\left(\frac{1}{r}\frac{\partial^2 w}{\partial r \partial \theta} - \frac{1}{r^2}\frac{\partial w}{\partial \theta}\right). \tag{3}$$

where $w(r,\theta)$ denote transverse displacements. The shear forces can be expressed as follows (cf. Timoshenko and Woinowsky-Krieger 1959)

$$Q_r = -D\frac{\partial}{\partial r}\left(\Delta w\right) \quad \text{and} \quad Q_\theta = -D\frac{\partial\left(\Delta w\right)}{r\partial\theta}, \tag{4}$$

where

$$\Delta w = \frac{\partial^2 w}{\partial r^2} + \frac{1}{r}\frac{\partial w}{\partial r} + \frac{1}{r^2}\frac{\partial^2 w}{\partial \theta^2}. \tag{5}$$

The free boundary conditions on the hole boundary can be written in the form

$$V_r|_{r=\rho} = \left.\left(Q_r - \frac{\partial M_{r\theta}}{r\partial\theta}\right)\right|_{r=\rho} = 0, \qquad M_{rr}|_{r=\rho} = 0. \tag{6}$$

2.2 Displacement and bending moment fields in plates: uniform and weakened by a hole

2.2.1 Uniform elastic plate under biaxial bending

Let us assume, that at the point $\mathbf{x}(0;0)$ of the plate without hole the principal moments $M_1 = M_{x_1}$, $M_2 = M_{x_2}$ occur in directions x_1, x_2 (Fig. 2a). Using polar coordinates, the displacement field in the neighborhood of the point $\mathbf{x}$ (cf. Timoshenko and Woinowsky-Krieger 1959) can be presented in the form

$$w^{(0)}\left(r,\theta\right) = w_0 - \frac{\left(M_1+M_2\right)r^2}{4D\left(1+\nu\right)} - \frac{\left(M_1-M_2\right)r^2}{4D\left(1-\nu\right)}\cos 2\theta, \tag{7}$$

where $w_0 = w^{(0)}(0;0)$ denotes displacement at the center of the coordinate system. In view of the relations (2), (3) formulas for distribution of moments $M_{rr}^{(0)}$, $M_{\theta\theta}^{(0)}$, $M_{r\theta}^{(0)}$ take the form

$$M_{rr}^{(0)}\left(r,\theta\right) = \frac{M_1+M_2}{2} + \frac{M_1-M_2}{2}\cos 2\theta, \tag{8}$$

$$M_{\theta\theta}^{(0)}\left(r,\theta\right) = \frac{M_1+M_2}{2} - \frac{M_1-M_2}{2}\cos 2\theta, \tag{9}$$

$$M_{r\theta}^{(0)}\left(r,\theta\right) = \frac{M_1-M_2}{2}\sin 2\theta. \tag{10}$$

2.2.2 Elastic plate with hole under biaxial bending

Now, let us assume, that at the point $\mathbf{x}(0;0)$ an infinitesimally small hole of radius ρ is introduced. The principal moments $M_1 = M_{x_1}$, $M_2 = M_{x_2}$, as previously occur in directions x_1, x_2 (Fig. 2b). Then, the displacement field

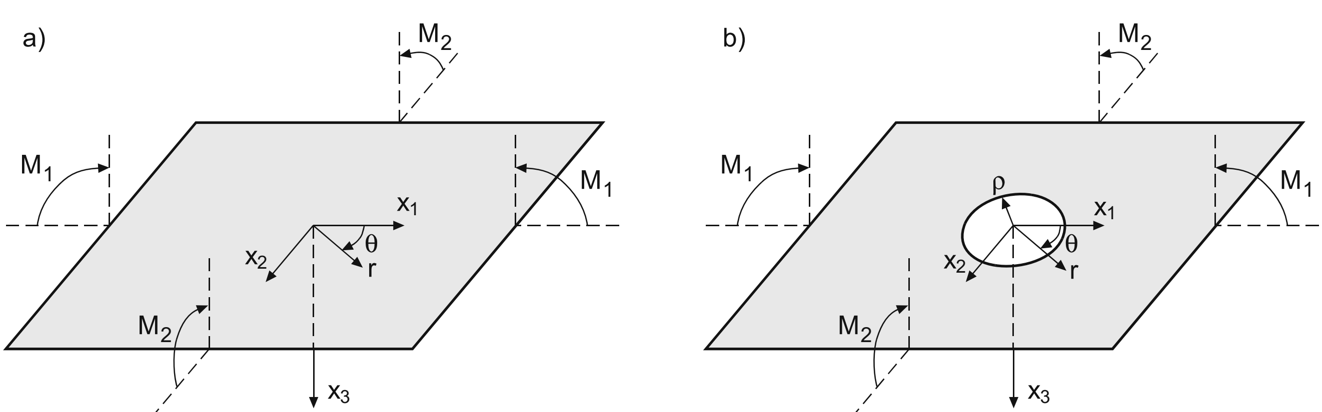

Fig. 2 Infinitesimally small element of the primary plate: **a** without hole; **b** with hole

in the neighborhood of the hole (cf. Timoshenko and Woinowsky-Krieger 1959) can be presented in the form

$$w(r,\theta) = w_0 - \frac{(M_1+M_2)\,r^2}{4D(1+\nu)} - \frac{(M_1-M_2)\,r^2}{4D(1-\nu)}\cos 2\theta + \\ -\frac{(M_1+M_2)\,\rho^2}{2D}A\ \ln r \\ -\frac{(M_1-M_2)\,\rho^2}{2D}\left(B+C\frac{\rho^2}{r^2}\right)\cos 2\theta, \qquad (11)$$

where three unknown constants A, B, C occur. The values of these constants can be determined using the boundary conditions (6), so we have

$$A=\frac{1}{1-\nu},\quad B=\frac{1}{3+\nu},\quad C=-\frac{1}{2(3+\nu)}. \qquad (12)$$

Now, using relations (2), (3), the formulas for distribution of moments M_{rr}, $M_{\theta\theta}$, $M_{r\theta}$ in the neighborhood of the hole take the form

$$M_{rr}(r,\theta)=\frac{M_1+M_2}{2}\left(1-\frac{\rho^2}{r^2}\right)+\frac{M_1-M_2}{2} \\ \times\left(1-\frac{4\nu}{3+\nu}\frac{\rho^2}{r^2}-\frac{3-3\nu}{3+\nu}\frac{\rho^4}{r^4}\right)\cos 2\theta, \quad (13)$$

$$M_{\theta\theta}(r,\theta)=\frac{M_1+M_2}{2}\left(1+\frac{\rho^2}{r^2}\right)-\frac{M_1-M_2}{2} \\ \times\left(1+\frac{4}{3+\nu}\frac{\rho^2}{r^2}-\frac{3-3\nu}{3+\nu}\frac{\rho^4}{r^4}\right)\cos 2\theta, \quad (14)$$

$$M_{r\theta}(r,\theta)=\frac{M_1-M_2}{2}\left(1-\frac{2-2\nu}{3+\nu}\frac{\rho^2}{r^2}+\frac{3-3\nu}{3+\nu}\frac{\rho^4}{r^4}\right)\sin 2\theta. \qquad (15)$$

It is easy to check, that $V_r|_{r=\rho}=0$, $M_{rr}|_{r=\rho}=0$, while values of the moments $M_{\theta\theta}$, $M_{r\theta}$ on the boundary of the hole are equal to

$$M_{\theta\theta}|_{r=\rho}=(M_1+M_2)-\alpha\,(M_1-M_2)\cos 2\theta, \quad \text{where} \\ \alpha=\frac{2(1+\nu)}{3+\nu}, \qquad (16)$$

$$M_{r\theta}|_{r=\rho}=\beta\,(M_1-M_2)\sin 2\theta, \quad \text{where} \quad \beta=\frac{2}{3+\nu}. \qquad (17)$$

Let us notice, that each expression for distribution of moments can be presented as the sum of terms corresponding to solution of the plate without hole derived in Section 2.2.1 and of the additional terms responsible for introduction of the hole. Moreover, for $r\neq 0$ the following relationships occur

$$w(r,\theta)|_{\rho=0}=w^{(0)}(r,\theta) \qquad (18)$$

and

$$M_{rr}(r,\theta)|_{\rho=0}=M_{rr}^{(0)}(r,\theta), \\ M_{\theta\theta}(r,\theta)|_{\rho=0}=M_{\theta\theta}^{(0)}(r,\theta), \\ M_{r\theta}(r,\theta)|_{\rho=0}=M_{r\theta}^{(0)}(r,\theta). \qquad (19)$$

Similarly, in view of (2), we have

$$\kappa_{rr}(r,\theta)|_{\rho=0}=\kappa_{rr}^{(0)}(r,\theta), \\ \kappa_{\theta\theta}(r,\theta)|_{\rho=0}=\kappa_{\theta\theta}^{(0)}(r,\theta), \\ \kappa_{r\theta}(r,\theta)|_{\rho=0}=\kappa_{r\theta}^{(0)}(r,\theta), \qquad (20)$$

where $\kappa_{rr}^{(0)}$, $\kappa_{\theta\theta}^{(0)}$, $\kappa_{r\theta}^{(0)}$ are the curvatures for the uniform plate, while κ_{rr}, $\kappa_{\theta\theta}$, $\kappa_{r\theta}$ denote the curvatures for the plate with hole.

2.3 Variational formulation of the topological derivative for a functional of curvatures and displacements

Consider the case when a functional of curvatures

$$\boldsymbol{\kappa}=[\kappa_{11},\kappa_{22},\kappa_{12}]^T=\left[-\frac{\partial^2 w}{\partial x_1^2},-\frac{\partial^2 w}{\partial x_2^2},-2\frac{\partial^2 w}{\partial x_2\partial x_1}\right]^T \qquad (21)$$

and transverse displacements w is of the form

$$G=\int_{A_\rho}F(\boldsymbol{\kappa})dA+\int_{A_\rho}f(w)\,dA. \qquad (22)$$

Let us notice, that in view of (18), (20), we have

$$\lim_{\rho\to 0}G=G^*, \qquad (23)$$

where $G^*=\int_A F\left(\boldsymbol{\kappa}^{(0)}\right)dA+\int_A f\left(w^{(0)}\right)dA$ denotes a value of the functional for the uniform plate. It means, that the topological derivative of the functional G^*

dependent on the fields $\boldsymbol{\kappa}^{(0)} = \left[\kappa_{11}^{(0)}, \kappa_{22}^{(0)}, \kappa_{12}^{(0)}\right]^T$ and $w^{(0)}$ for the uniform plate can be treated as the topological derivative of the functional G defined by (22).

The first variation of this functional with respect to expansion of an infinitesimally small hole of radius ρ introduced at the point $\mathbf{x}$ can be presented as follows

$$\delta G = \int\limits_{A_\rho} \frac{\partial F}{\partial \boldsymbol{\kappa}} \cdot \delta\boldsymbol{\kappa}\ dA + \int\limits_{A_\rho} \frac{\partial f}{\partial w} \delta w dA + \sum_{k=1}^{2} \int\limits_{\Gamma_\rho} (F + f)\, n_k \delta\varphi_k d\Gamma_\rho, \tag{24}$$

where $\mathbf{n} = [n_1, n_2]^T$ is the unit vector normal to the boundary Γ_ρ of the hole, $\delta\boldsymbol{\varphi} = [\delta\varphi_1, \delta\varphi_2]^T$ is the vector function of shape transformation of the hole and $(\cdot)$ denotes the scalar product. Let us introduce an adjoint plate subjected to initial bending moments $\mathbf{M}^{ai} = \left[M_{11}^{ai}, M_{22}^{ai}, M_{12}^{ai}\right]^T$ and transverse load p^{a0}, namely

$$\mathbf{M}^{ai} = \mathbf{D}\boldsymbol{\kappa}^{ai} = \frac{\partial F}{\partial \boldsymbol{\kappa}} \text{ in } A_\rho, \quad p^{a0} = \frac{\partial f}{\partial w} \text{ in } A_\rho. \tag{25}$$

The field of initial moments $\mathbf{M}^{ai}$ induces a field of global moments $\mathbf{M}^a = \mathbf{D}\boldsymbol{\kappa}^a$ in the form

$$\mathbf{M}^a = \mathbf{M}^{ai} + \mathbf{M}^{ar}, \tag{26}$$

where $\mathbf{M}^{ar}$ denotes field of the elastic moments, $\boldsymbol{\kappa}^a$ is the adjoint plate curvature field and $\mathbf{D}$ is the elastic stiffness matrix. The initial moment $\mathbf{M}^{ai}$ is induced by the initial curvature field $\boldsymbol{\kappa}^{ai}$ not satisfying the compatibility condition, so the field of elastic moments $\mathbf{M}^{ar}$ satisfies the equilibrium conditions for the loading specified by (25). Moreover, the support conditions on the boundary Γ of the adjoint plate are the same as those of the primary plate (cf. Dems and Mróz 1989). Now, taking into account (25) and the relationship $\sum\limits_{k=1}^{2} n_k \delta\varphi_k = -\delta\rho$, (24) becomes

$$\delta G = \int\limits_{A_\rho} \mathbf{M}^{ai} \cdot \delta\boldsymbol{\kappa}\ dA + \int\limits_{A_\rho} p^{a0} \delta w dA - \int\limits_{\Gamma_\rho} (F + f)\, \delta\rho d\Gamma_\rho. \tag{27}$$

Now, the virtual work equation is

$$\int\limits_{A_\rho} \mathbf{M}^{ar} \cdot \delta\boldsymbol{\kappa}\ dA = \int\limits_{A_\rho} p^{a0} \delta w dA, \tag{28}$$

and the complementary virtual work equation takes the form

$$\int\limits_{A_\rho} \mathbf{M}^a \cdot \delta\boldsymbol{\kappa}\ dA = \int\limits_{A_\rho} \boldsymbol{\kappa}^a \cdot \delta\mathbf{M}\ dA = \int\limits_{\Gamma_\rho} \mathbf{M} \cdot \boldsymbol{\kappa}^a \delta\rho d\Gamma_\rho - \int\limits_{\Gamma_\rho} p^0 w^a \delta\rho d\Gamma_\rho, \tag{29}$$

where w^a is the adjoint plate deflection field. Equation (29) results from the observation that $\delta\mathbf{M} = -\mathbf{M}$ and $\delta\mathbf{p}^0 = -\mathbf{p}^0$ over the hole area. In view of (26), (28), (29), the first variation (27) of the functional G takes the form

$$\delta G = \int\limits_{\Gamma_\rho} \left(\mathbf{M} \cdot \boldsymbol{\kappa}^a - F - f - p^0 w^a\right) d\Gamma_\rho \delta\rho. \tag{30}$$

Let us introduce the polar coordinates r, θ with the origin at the center of the hole (Fig. 1). Taking into account, that $\delta G = \frac{\partial G}{\partial \rho}\delta\rho$ and applying integration with respect to θ, (30) can be rewritten as follows

$$\frac{\partial G}{\partial \rho} = \int\limits_0^{2\pi} \left(\mathbf{M} \cdot \boldsymbol{\kappa}^a - F - f - p^0 w^a\right) \rho d\theta. \tag{31}$$

It is easy to notice that the first derivative with respect to hole radius for $\rho = 0$ is equal to zero. In order to determine the topological derivative with respect to hole area $A = \pi\rho^2$ at the point $\mathbf{x}$, we use the following relationship

$$T^G_{,A_0}(\mathbf{x}) = \left.\left(\frac{\partial G}{\partial \rho}\frac{\partial \rho}{\partial A}\right)\right|_{\rho=0}. \tag{32}$$

Taking into account, that $dA = 2\pi\rho d\rho$ and substituting (31) into (32), the topological derivative can be expressed in the form

$$T^G_{,A_0}(\mathbf{x}) = \frac{1}{2\pi} \int\limits_0^{2\pi} \left(\mathbf{M} \cdot \boldsymbol{\kappa}^a - F - f - p^0 w^a\right) d\theta. \tag{33}$$

In order to obtain the final formula for topological derivative, we need to determine distribution of moments (curvatures) on the boundary of hole in the primary and adjoint structures.

2.4 Adjoint plate with hole under biaxial bending

Let us assume, that at the point $\mathbf{x}(0;0)$ of the adjoint plate, where the infinitesimally small hole of radius ρ

is introduced, the principal moments M_1^a, M_2^a occur. The angle between principal directions corresponding to moments M_1 and M_1^a is denoted by χ (Fig. 3). Now, analogously as in the case of the primary plate, distributions of moments $M_{\theta\theta}^a$, $M_{r\theta}^a$ in the adjoint plate and their values on the boundary of the hole are

$$M_{rr}^a(r,\theta)=\frac{M_1^a+M_2^a}{2}\left(1-\frac{\rho^2}{r^2}\right)+\frac{M_1^a-M_2^a}{2}\times\left(1-\frac{4\nu}{3+\nu}\frac{\rho^2}{r^2}-\frac{3-3\nu}{3+\nu}\frac{\rho^4}{r^4}\right)\cos 2(\theta-\chi), \tag{34}$$

$$M_{\theta\theta}^a(r,\theta)=\frac{M_1^a+M_2^a}{2}\left(1+\frac{\rho^2}{r^2}\right)-\frac{M_1^a-M_2^a}{2}\times\left(1+\frac{4}{3+\nu}\frac{\rho^2}{r^2}-\frac{3-3\nu}{3+\nu}\frac{\rho^4}{r^4}\right)\cos 2(\theta-\chi), \tag{35}$$

$$M_{r\theta}^a(r,\theta)=\frac{M_1^a-M_2^a}{2}\left(1-\frac{2-2\nu}{3+\nu}\frac{\rho^2}{r^2}+\frac{3-3\nu}{3+\nu}\frac{\rho^4}{r^4}\right)\times\sin 2(\theta-\chi), \tag{36}$$

$$M_{\theta\theta}^a\big|_{r=\rho}=\left(M_1^a+M_2^a\right)-\alpha\left(M_1^a-M_2^a\right)\cos 2(\theta-\chi), \tag{37}$$

$$M_{r\theta}^a\big|_{r=\rho}=\beta\left(M_1^a-M_2^a\right)\sin 2(\theta-\chi), \tag{38}$$

while in accordance with the boundary conditions (6) there is $V_r^a\big|_{r=\rho}=0$ and $M_{rr}^a\big|_{r=\rho}=0$.

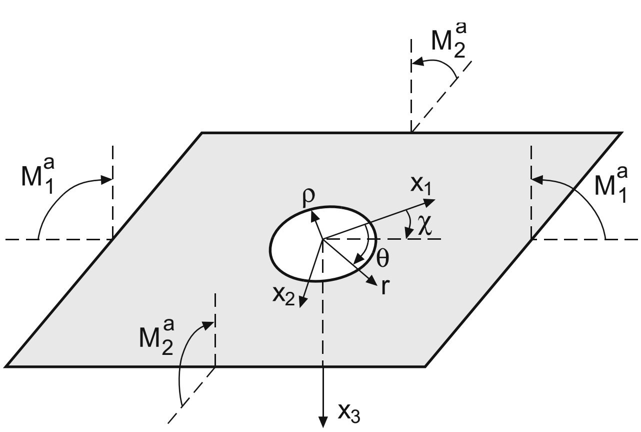

Fig. 3 Infinitesimally small element of the adjoint plate

2.5 Topological derivative for a functional of curvatures and displacements

We can note, that for the adjoint plate the relations analogous to (2–6) are also valid. Then, we get the following relationships

$$\kappa_{rr}^a\big|_{r=\rho}=-\nu\,\kappa_{\theta\theta}^a\big|_{r=\rho}\quad\text{and}\quad\kappa_{\theta\theta}^a\big|_{r=\rho}=\left.\frac{M_{\theta\theta}^a}{D\left(1-\nu^2\right)}\right|_{r=\rho}. \tag{39}$$

Now taking into account (2), (6), (39), the topological derivative (33) of the analyzed functional G takes the form

$$T_{,A_0}^G(\mathbf{x})=\frac{1}{2\pi D\left(1-\nu^2\right)}\int_0^{2\pi}M_{\theta\theta}M_{\theta\theta}^a d\theta+\frac{1}{\pi D(1-\nu)}\int_0^{2\pi}M_{r\theta}M_{r\theta}^a d\theta-\frac{1}{2\pi}\int_0^{2\pi}F\left(M_{\theta\theta},M_{r\theta}\right)d\theta-\frac{1}{2\pi}\int_0^{2\pi}\left(f+p^0w^a\right)d\theta, \tag{40}$$

where $F(M_{\theta\theta}, M_{r\theta})$ corresponds to the function $F(\boldsymbol{\kappa})$ expressed on the boundary of the hole in terms of the moments $M_{\theta\theta}$, $M_{r\theta}$.

Next, we will determine values of the two first terms on the right hand side of (40). Taking into account (16), (17), (37), (38), we obtain

$$\int_0^{2\pi}M_{\theta\theta}M_{\theta\theta}^a d\theta=2\pi\left[\left(M_1+M_2\right)\left(M_1^a+M_2^a\right)+\frac{1}{2}\alpha^2\left(M_1-M_2\right)\left(M_1^a-M_2^a\right)\cos 2\chi\right], \tag{41}$$

and

$$\int_0^{2\pi}M_{r\theta}M_{r\theta}^a d\theta=\pi\beta^2\left(M_1-M_2\right)\left(M_1^a-M_2^a\right)\cos 2\chi. \tag{42}$$

Moreover, we have

$$\int_0^{2\pi} \left[f(w) + p^0 w^a \right] d\theta = 2\pi \left[f(w_0) + p^0 w_0^a \right], \tag{43}$$

where $w_0^a = w^{(0)a}(0; 0)$ denotes displacement of the unmodified adjoint plate at the point $\mathbf{x}$.

Finally, taking into account (41), (42), (43) in (40), the topological derivative with respect to introduction of an infinitesimally small hole at the point $\mathbf{x}$ of the Kirchhoff's plate can be presented in the form

$$\begin{aligned} T^G_{,A_0}(\mathbf{x}) = \frac{12}{Eh^3} \Bigg[&(M_1 + M_2)\left(M_1^a + M_2^a\right) \\ &+ \frac{2(1+\nu)}{3+\nu}(M_1 - M_2)\left(M_1^a - M_2^a\right) cos 2\chi \Bigg] \\ &- \frac{1}{2\pi}\int_0^{2\pi} F(M_{\theta\theta}, M_{r\theta})\, d\theta - f(w_0) - p^0 w_0^a, \end{aligned} \tag{44}$$

where the expression $\int_0^{2\pi} F(M_{\theta\theta}, M_{r\theta})\, d\theta$ should be determined separately for each form of the function F. In the case, when the functional (22) corresponds to the strain energy U, the problem becomes self-adjoint. Moreover, assuming that $f = 0$ and $p^0 = 0$ on boundary Γ_ρ of a new hole, the topological derivative (44) can be rewritten as follows (cf. Novotny et al. 2005)

$$T^U_{,A_0}(\mathbf{x}) = \frac{6}{Eh^3}\left[(M_1 + M_2)^2 + \frac{2(1+\nu)}{3+\nu}(M_1 - M_2)^2 \right]. \tag{45}$$

2.6 Topological derivative for a functional of bending moments and reactions

Now, let us consider the following functional of moments and reactions

$$G = \int_{A_\rho} H(\mathbf{M})\, dA + \int_{\Gamma_u} g(\mathbf{T})\, d\Gamma_u, \tag{46}$$

where $H(\mathbf{M})$ is the function of moments $\mathbf{M} = [M_{11}, M_{22}, M_{12}]^T$ and $g(\mathbf{T})$ denotes function of reaction forces acting on boundary Γ_u $(\Gamma_u \subset \Gamma)$. In this case the adjoint structure is specified by the relations

$$\boldsymbol{\kappa}^{ai} = \frac{\partial H}{\partial \mathbf{M}}, \quad p^{a0} = 0 \text{ in } A_\rho, \quad \mathbf{u}^{a0} = -\frac{\partial g}{\partial \mathbf{T}} \text{ on } \Gamma_u, \tag{47}$$

where $\boldsymbol{\kappa}^{ai}$ are the initial curvatures. The field of the initial curvatures induces the field of global curvatures in the form $\boldsymbol{\kappa}^a = \boldsymbol{\kappa}^{ai} + \boldsymbol{\kappa}^{ar}$, where $\boldsymbol{\kappa}^{ar}$ is the field of the elastic curvatures. Moreover, $\mathbf{u}^{a0}$ denotes the generalized displacements corresponding to the reactions $\mathbf{T}$. Now, in view of (47), sensitivity of the functional (46) with respect to introduction of a hole of infinitesimally small radius ρ at point $\mathbf{x}$, can be expressed analogously to (27), namely

$$\delta G = \int_{A_\rho} \boldsymbol{\kappa}^{ai} \cdot \delta \mathbf{M} dA - \int_{\Gamma_u} \mathbf{u}^{a0} \cdot \delta \mathbf{T} d\Gamma_u - \int_{\Gamma_\rho} H d\Gamma_\rho \delta\rho, \tag{48}$$

where Γ_ρ denotes boundary of this hole. So, in view of the virtual work equation

$$\int_{A_\rho} \boldsymbol{\kappa}^{ar} \cdot \delta \mathbf{M} dA = \int_{A_\rho} \mathbf{M}^{ar} \cdot \delta \boldsymbol{\kappa} dA = \int_{A_\rho} p^{a0} \delta w dA = 0, \tag{49}$$

and the complementary virtual work equation

$$\begin{aligned} \int_{A_\rho} \boldsymbol{\kappa}^a \cdot \delta \mathbf{M} dA = \int_{\Gamma_\rho} \mathbf{M} \cdot \boldsymbol{\kappa}^a d\Gamma_\rho \delta\rho + \int_{\Gamma_u} \mathbf{u}^{a0} \cdot \delta \mathbf{T} d\Gamma_u \\ - \int_{\Gamma_\rho} p^0 w^a d\Gamma_\rho \delta\rho, \end{aligned} \tag{50}$$

next of the relation $\delta G = \frac{\partial G}{\partial \rho}\delta\rho$, the first derivative of the functional (46) takes the form

$$\frac{\partial G}{\partial \rho} = \int_0^{2\pi} \left(\mathbf{M} \cdot \boldsymbol{\kappa}^a - H - p^0 w^a \right) \rho d\theta. \tag{51}$$

Now, taking into account (32), the topological derivative of the considered functional with respect to the hole area is

$$T^G_{,A_0}(\mathbf{x}) = \frac{1}{2\pi}\int_0^{2\pi} \left(\mathbf{M} \cdot \boldsymbol{\kappa}^a - H - p^0 w^a \right) d\theta. \tag{52}$$

Finally, following the previous derivation, the topological derivative of the functional of static fields (46) can be written as follows

$$T^{G}_{,A_0}(\mathbf{x}) = \frac{12}{Eh^3}\left[(M_1+M_2)\left(M_1^a+M_2^a\right)+\frac{2(1+\nu)}{3+\nu}\right.$$
$$\left.\times\,(M_1-M_2)\left(M_1^a-M_2^a\right)\cos 2\chi\right]$$
$$-\frac{1}{2\pi}\int_0^{2\pi} H\left(M_{\theta\theta}, M_{r\theta}\right)d\theta - p^0 w_0^a, \qquad (53)$$

where the expression $\int_0^{2\pi} H\left(M_{\theta\theta}, M_{r\theta}\right)d\theta$ should be determined separately for each form of the function H.

2.7 Topological derivative of the cost functional

Now, let us consider the topological derivative of the global cost C. When we assume, that the cost of the structure is proportional to the material volume, it can be expressed as follows

$$C = c\left(V_0 - \pi\rho^2 h\right), \qquad (54)$$

where c is a unit cost, V_0 denotes initial volume of the considered structure, and, as previously, h denotes its thickness and ρ is the radius of the inserted small hole. Thus, the topological derivative of the cost functional with respect to introduction of this infinitesimally small hole, takes the form

$$T^{C}_{,A_0}(\mathbf{x}) = \left.\left(\frac{\partial C}{\partial\rho}\frac{\partial\rho}{\partial A}\right)\right|_{\rho=0} = -ch. \qquad (55)$$

3 Topological derivative with respect to introduction of ribs into plate

The analysis presented in this section is based on the results obtained in the paper by Bojczuk and Szteleblak (2008). We shall consider an elastic plate made of isotropic material, which after rib introduction behaves as the orthotropic structure.

3.1 Topological derivative for functional of curvatures and displacements

Now, the constitutive relations for the plate in the principal directions of orthotropy are

$$\mathbf{M} = \mathbf{D}^0\boldsymbol{\kappa}. \qquad (56)$$

They can also be presented in the extended form as follows

$$\begin{bmatrix} M_{11} \\ M_{22} \\ M_{12} \end{bmatrix} = \begin{bmatrix} D^0_{11} & D^0_{12} & 0 \\ D^0_{21} & D^0_{22} & 0 \\ 0 & 0 & D^0_{66} \end{bmatrix}\begin{bmatrix} \kappa_{11} \\ \kappa_{22} \\ \kappa_{12} \end{bmatrix}, \qquad (57)$$

where $\mathbf{D}^0$ denotes the bending stiffness matrix. Assume that on the interface S_C separating rib and remaining part of the plate, the continuity conditions can be presented as follows

$$[w] = 0,\quad [\kappa_{11}] = [\kappa_{tt}] = 0\quad [M_{22}] = [M_{nn}] = 0,$$
$$[M_{21}] = [M_{nt}] = 0, \qquad (58)$$

where the last condition also can be assumed in the form (cf. Woźniak 2001)

$$[\kappa_{21}] = [\kappa_{nt}] = 0. \qquad (59)$$

Moreover, [ ] denotes the jump of the enclosed quantity on S_C calculated as a difference of the respective values in the plate and in the rib. Now, using homogenization theory (cf. Lewiński and Telega 2000; Woźniak 2001), the average stiffnesses of the plate in domain collaborating with the rib, which is specified by dimension a, take the form

$$D^0_{11} = \frac{E}{12}\frac{a_1h_1^3 + a_2h_3^3}{a} + \frac{E\nu^2}{12\left(1-\nu^2\right)}\frac{a}{\frac{a_1}{h_1^3}+\frac{a_2}{h_3^3}},$$

$$D^0_{22} = \frac{E}{12\left(1-\nu^2\right)}\frac{a}{\frac{a_1}{h_1^3}+\frac{a_2}{h_3^3}},$$

$$D^0_{12} = D^0_{21} = \nu D^0_{22},$$

$$D^0_{66} = \frac{1-\nu}{2}D^0_{22} = \frac{E}{24(1+\nu)}\frac{a}{\frac{a_1}{h_1^3}+\frac{a_2}{h_3^3}}, \qquad (60)$$

where a_2 denotes the width of the rib, $a_1 = a - a_2$, while h_3 ($h_3 = h_1 + 2h_2$) is the total height of the rib, which is equal to the sum of the plate thickness h_1 and two one-sided rib heights h_2 (Fig. 4).

Let us consider the functional of curvatures and displacements (22). We choose as the topological design parameter the width of the rib a_2 and the topological derivative should be determined for $a_2 = 0$. Now, using

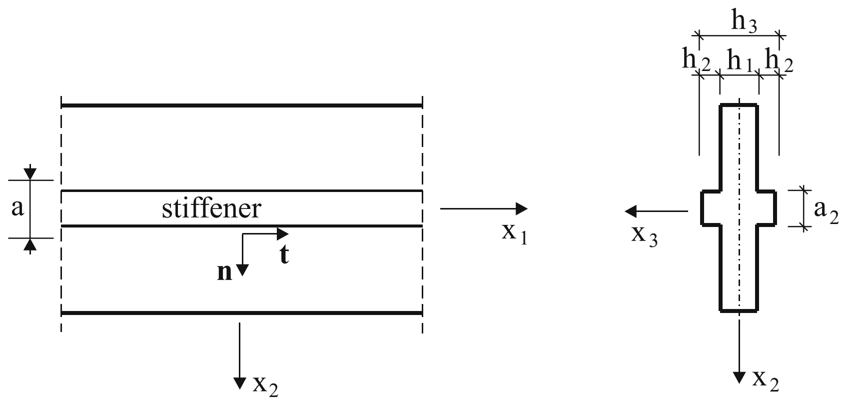

Fig. 4 Geometry of the plate reinforced by the rib

the adjoint method, where adjoint plate is defined analogously as in Section 2, the topological derivative of the functional (22) with respect to introduction of the rib along line l defining position of the rib, takes the form

$$T^G_{,a_2}(l) = \left.\frac{\partial G}{\partial a_2}\right|_{a_2=0} = \int_{A_m}\left(\left.\frac{\partial F}{\partial a_2}\right|_{a_2=0} - \boldsymbol{\kappa}^T \left.\frac{\partial \mathbf{D}^0}{\partial a_2}\right|_{a_2=0}\boldsymbol{\kappa}^a\right)dA_m$$

$$= a\int_l\left(\left.\frac{\partial F}{\partial a_2}\right|_{a_2=0} - \boldsymbol{\kappa}^T \left.\frac{\partial \mathbf{D}^0}{\partial a_2}\right|_{a_2=0}\boldsymbol{\kappa}^a\right)dl, \tag{61}$$

where A_m denotes the domain (zone) collaborating with the rib, of the shape of narrow strip. Here, l is the line defining position of the rib and a denotes the width of this strip. It is assumed, that the considered modification can be treated as replacement of primary, isotropic material in the zone by material with structural orthotropy induced by introduction of rib. As the width of this zone is small, the respective integral with respect to the domain A_m can be substituted by integral along line l coincident with virtual rib.

Taking into account, that derivatives of the components of the stiffness matrix $\mathbf{D}^0$ are of the form

$$\left.\frac{\partial D^0_{11}}{\partial a_2}\right|_{a_2=0} = \frac{E}{12a\left(1-\nu^2\right)}\left(h_3^3 - h_1^3\right)\left(1-\nu^2+\frac{h_1^3}{h_3^3}\nu^2\right),$$

$$\left.\frac{\partial D^0_{22}}{\partial a_2}\right|_{a_2=0} = \frac{E}{12a\left(1-\nu^2\right)}\left(h_3^3 - h_1^3\right)\frac{h_1^3}{h_3^3},$$

$$\left.\frac{\partial D^0_{12}}{\partial a_2}\right|_{a_2=0} = \nu\left.\frac{\partial D^0_{22}}{\partial a_2}\right|_{a_2=0},$$

$$\left.\frac{\partial D^0_{66}}{\partial a_2}\right|_{a_2=0} = \frac{1-\nu}{2}\left.\frac{\partial D^0_{22}}{\partial a_2}\right|_{a_2=0}, \tag{62}$$

the topological derivative (61) finally can be presented as follows

$$T^G_{,a_2}(l) = \left.\frac{\partial \mathrm{G}}{\partial a_2}\right|_{a_2=0}$$

$$= \int_l\left[a\left.\frac{\partial F}{\partial a_2}\right|_{a_2=0} - D_r\left(1-\nu^2+\frac{h_1^3}{h_3^3}\nu^2\right)\kappa_{11}\kappa^a_{11}\right.$$

$$- D_r\frac{h_1^3}{h_3^3}\kappa_{22}\kappa^a_{22} - \nu D_r\frac{h_1^3}{h_3^3}\left(\kappa_{11}\kappa^a_{22}+\kappa_{22}\kappa^a_{11}\right)$$

$$\left. - D_r\frac{1-\nu}{2}\frac{h_1^3}{h_3^3}\kappa_{12}\kappa^a_{12}\right]dl, \tag{63}$$

where $D_r = \frac{E}{12\left(1-\nu^2\right)}\left(h_3^3 - h_1^3\right)$. More details of this approach is presented in Bojczuk and Szteleblak (2008).

A similar topological sensitivity analysis can be presented for functionals of moments and reactions. Analogous considerations can also be formulated for problems of introduction of stiffening fibers.

3.2 Topological derivative of the cost functional

Now, let us consider cost functional expressed as follows

$$C = C_\mathrm{m} + C_\mathrm{r}, \tag{64}$$

where C_m denotes the total cost of the material and C_r is the installation cost of the rib. The material cost is the sum of the plate material cost and rib material cost, namely

$$C_\mathrm{m} = c\left(V_\mathrm{d}+V_\mathrm{r}\right) = c\left(\int_A h_1 dA + 2a_2\int_l h_2 dl\right), \tag{65}$$

where c is the unit cost of the plate and rib material, V_d denotes the volume of the unmodified plate and V_r the volume of the introduced rib. The installation cost of the rib can be written in the following form

$$C_{\mathrm{r}} = c_{\mathrm{r}} V_{\mathrm{r}} = 2 c_{\mathrm{r}} a_2 \int\limits_l h_2 dl, \tag{66}$$

where c_{r} denotes the unit installation cost.

Assuming, as previously, that the rib width a_2 is the design parameter, the sensitivity of the cost functional can be presented as follows

$$T^C_{,a_2}(l) = \left.\frac{\partial C}{\partial a_2}\right|_{a_2=0} = 2\left(c + c_{\mathrm{r}}\right) \int\limits_l h_2 dl, \text{ or when}$$

$$h_2 = \text{const} \quad T^C_{,a_2}(l) = \left.\frac{\partial C}{\partial a_2}\right|_{a_2=0} = 2 h_2 l \left(c + c_{\mathrm{r}}\right). \tag{67}$$

4 Heuristic algorithms of plate optimization

Consider a general optimization problem of the form

$$\min\ G, \quad \text{subject to} \quad C - C_0 \leq 0, \tag{68}$$

where G is the objective functional (function), C denotes the global cost and C_0 is the upper bound on the global cost. Introducing the Lagrangian

$$L = G + \lambda \left(C - C_0\right), \tag{69}$$

where $\lambda \geq 0$, the optimality conditions with respect to design parameters p_i can be presented in the form

$$\frac{\partial G}{\partial p_i} + \lambda \frac{\partial C}{\partial p_i} = 0, \qquad i = 1, 2, \ldots, r,$$
$$\lambda \left(C - C_0\right) = 0. \tag{70}$$

The optimal values of the design parameters and of Lagrange multiplier λ can be determined in the incremental process of gradient optimization. Next, we try to introduce topology modification. So, the condition of introduction of an infinitesimally small topology variation can be presented in the form

$$T^L_{,s} = T^G_{,s} + \lambda T^C_{,s} < 0, \tag{71}$$

where $T^L_{,s}$, $T^G_{,s}$, $T^C_{,s}$ are the topological derivatives, respectively of the Lagrangian, objective functional G and cost functional C with respect to topological parameter s at the point corresponding to the structure with unchanged topology. When the condition (71) is satisfied, the modification is introduced. Next, additional standard optimization with respect to design parameters p_i should be performed, where parameters describing new topological element should be added.

4.1 Algorithm of topology and shape optimization of plates

In the case of topology and shape optimization of plates, the condition (71) of introduction of infinitesimally small circular hole of area A_0 at the arbitrary point $\mathbf{x}$, using the concept of the topological derivative, takes the form

$$T^L_{,A_0}(\mathbf{x}) = T^G_{,A_0}(\mathbf{x}) + \lambda T^C_{,A_0}(\mathbf{x}) < 0, \tag{72}$$

where $T^L_{,A_0}(\mathbf{x})$, $T^G_{,A_0}(\mathbf{x})$, $T^C_{,A_0}(\mathbf{x})$ are the topological derivatives, respectively of the Lagrangian L, objective functional G (see (44), (45) and (53)) and cost functional C (see (55)). Moreover, a new small hole should be introduced at a point, where $T^L_{,A_0}(\mathbf{x})$ attains a minimal value (cf. bubble method, Eschenauer et al. 1994). It means, that the topological derivative can also be used to localize position of modification.

However, in order to accelerate optimization process, a finite modification can be applied (cf. Mróz and Bojczuk 2003). Now, the problem consists in introduction of finite holes of unknown size and shape together with introduction of finite changes of other boundaries. It is assumed, that domains of relatively small values of the topological derivative of Lagrangian, which is expressed by (72), should be eliminated. It can be performed using the level-set method by removal of all domains, where this topological derivative is smaller than adequately chosen negative isovalue. However, an alternative approach can be used. Taking into account that for the considered redesign process there is $T^C_{,A_0}(\mathbf{x}) < 0$, the local condition of modification (72) can be rewritten in the form

$$\Lambda < \lambda, \quad \text{where} \quad \Lambda = \frac{T^G_{,A_0}(\mathbf{x})}{-T^C_{,A_0}(\mathbf{x})}. \tag{73}$$

Here Λ is the local measure of increment of the objective functional G per unit decrease of the cost C induced by introduction of a small hole. In order to determine finite domain A_f for which the condition

(73) is satisfied and Λ attains values smaller than the selected iso-value, the following auxiliary problem is formulated

$$\min_{A_f} \Lambda_f, \tag{74}$$

where

$$\Lambda_f = \frac{\mu\lambda + \Delta G}{\mu - \Delta C} = \frac{\mu\lambda + \int_{A_f} T^G_{,A_0}(\mathbf{x})\, dA}{\mu - \int_{A_f} T^C_{,A_0}(\mathbf{x})\, dA} = \frac{\mu\lambda + \bar{T}^G A_f}{\mu - \bar{T}^C A_f}, \tag{75}$$

is the specially constructed design quality function, while μ ($\mu > 0$) denotes the scaling factor controlling amount of removed domain A_f related with the respective iso-value. Here ΔG, ΔC are the evaluations of the corresponding finite increments induced by finite modification and $\bar{T}^G$, $\bar{T}^C$ denote the average values of the respective topological derivatives in the modification domain. The function Λ_f before modification equals to Lagrange multiplier λ. When $\mu \to 0$, only domain for which Λ attains minimum, denoted by $\Lambda^{\min}$, is eliminated. Then, modification usually corresponds to introduction of infinitesimally small hole, analogously as in the bubble method. It is important to note, that if the bigger value of μ is chosen, the bigger domain is eliminated (Fig. 5). In particular, when $\mu \to \infty$, the whole domain for which the condition (73) is satisfied, will be removed. The condition of finite topology transformation analogous to (73) and size of eliminated domain determined from (74) take the form

$$\Lambda_f^{\min} < \lambda, \quad \text{where } \Lambda_f^{\min} = \min_{A_f} \Lambda_f \quad \text{and}$$

$$A_f = -\frac{\mu\left(\lambda - \Lambda_f^{\min}\right)}{\bar{T}^G + \Lambda_f^{\min} \bar{T}^C}. \tag{76}$$

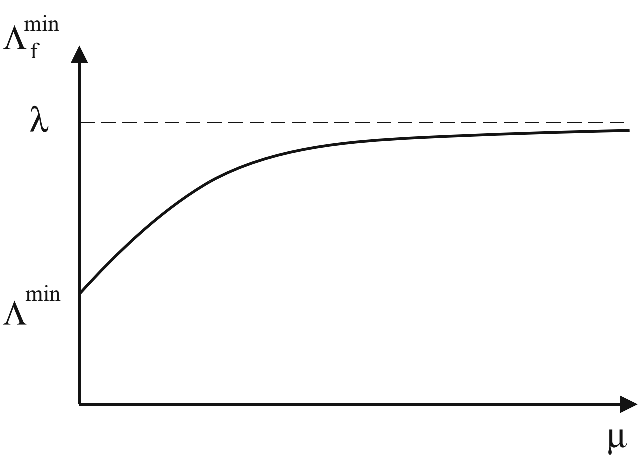

Fig. 5 Example relation between scaling factor μ and minimal value $\Lambda_f^{\min}$ of design quality function

Finally, the following algorithm of topology and shape optimization of plates can be proposed.

1. Formulate in detail optimization problem (68) and select initial design.
2. Specify the vector of dimensional and shape design parameters p_i.
3. Determine optimal values of the design parameters p_i and of Lagrange multiplier λ in order to satisfy optimality conditions (70) using arbitrary method of gradient optimization.
4. Calculate field of the topological derivative of Lagrangian $T^L_{,A_0}(\mathbf{x})$ in the domain of the structure.
5. In order to determine domain A_f, solve the problem (74).
6. Check the modification condition (76). If the condition is not satisfied, go to step 9.
7. Introduce finite modification by removal of the domain A_f and distribute material proportionally to the plate stiffness to achieve maximal global cost C_0.
8. Calculate new value of the objective function. If this value is smaller than the previous smallest value of the objective function, accept the modification and return to step 4, otherwise reject the modification.
9. If any finite modification is not introduced after the last execution of step 3 terminate optimization process. Otherwise update vector of dimensional and shape design parameters p_i and return to step 3.

4.2 Remarks about algorithm of optimization of stiffened plates

In the case of introduction of infinitesimally thin stiffeners lying along certain line l, the condition of modification acceptance can be presented analogously to (71) and (72), namely

$$T^L_{,a_2}(l) = T^G_{,a_2}(l) + \lambda T^C_{,a_2}(l) < 0, \tag{77}$$

where $T^L_{,a_2}(l)$, $T^G_{,a_2}(l)$, $T^C_{,a_2}(l)$ are the topological derivatives, respectively of the Lagrangian L, objective

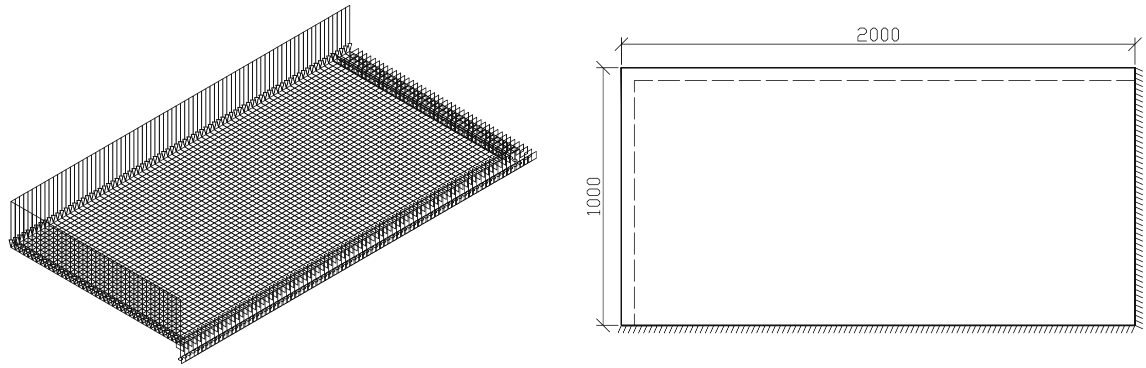

Fig. 6 Geometry, loading and boundary conditions of the analyzed plate

functional G (see (63)) and cost functional C (see (67)) with respect to width of rib a_2 at the point corresponding to zero width i.e. $a_2 = 0$. It is important to notice, that the line l should be chosen in such a way that $T^L_{,a_2}(l)$ attains minimum. For this purpose parameterization of this line using, for example, B-splines can be done. Now minimization problem takes the form

$$\min_{p_1, p_2, \dots p_r} T^L_{,a_2}(p_1, p_2, \dots, p_r), \tag{78}$$

where $p_i, i = 1,2,\dots,r$, are the parameters describing the line l.

Let us notice, that the algorithm of optimization of plates with stiffeners can be formulated analogously to the algorithm presented in Section 4.1. However, in this case auxiliary problem analyzed in point 5 corresponds to the problem (78). More details of this approach is presented in Bojczuk and Szteleblak (2008).

5 Illustrative examples

In this section numerical examples are discussed in order to show applicability and usefulness of heuristic algorithms presented in the previous section for problems of structural optimization.

5.1 Example: optimal design of topology and shape of plate

Consider the optimization problem (68) for the plate structure (2,000 mm × 1,000 mm) presented in Fig. 6 (cf. Bojczuk and Szteleblak 2005). Here, G corresponds to the elastic energy U and C denotes volume of the structure, while C_0 corresponds to the initial volume. The plate is clamped on two edges and loaded by uniformly distributed forces (5 kN/m) on two other edges. Structure is made of steel (Young's modulus is $E = 205$ GPa and Poisson's ratio $\nu = 0.3$). The initial

Fig. 7 Each third finite topology modification

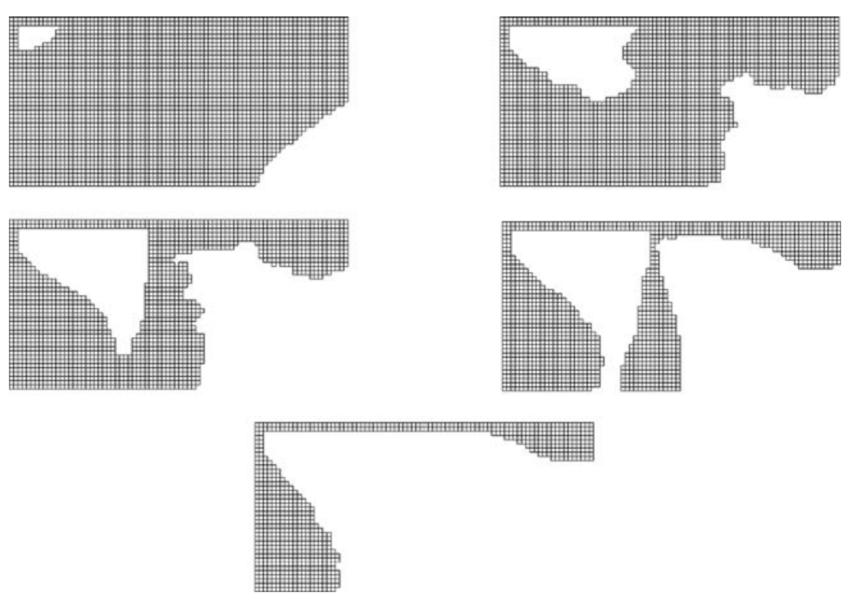

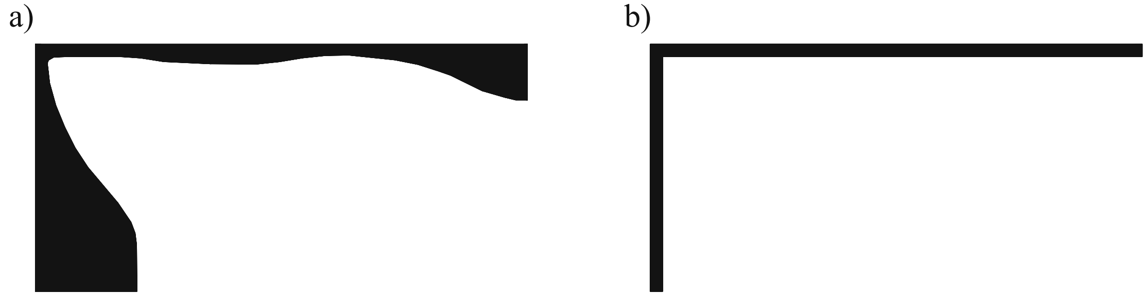

Fig. 8 Optimal designs: **a** the case with the condition imposed on the maximal thickness of the plate; **b** the case without thickness constraints

thickness of the plate is 10 mm. In order to avoid removal of loaded domain, geometrical constraints imposed on the design area are introduced. They are denoted by dashed line in Fig. 6. Also maximum thickness of the plate is limited to 50 mm.

In the present example, using solutions of the preliminary problem (74), successive finite topology modifications are introduced. Optimization process is stopped after 15 modifications (Fig. 7), when the constraints imposed on maximum thickness of the structure become active. Next, final correction of the shape is carried out and the optimal design is shown in Fig. 8a. The ratio of the strain energies of the initial and final design is $U^{(\mathrm{init})}/U^{(\mathrm{opt})} = 37.33$, while the corresponding ratio of the optimal and initial thickness is $h^{(\mathrm{opt})}/h^{(\mathrm{init})} = 5.00$.

In the case, when constraints imposed on thickness of the plate are not used, optimal design is determined by geometric constraints imposed on loaded area. Then, the optimal structure is the simple frame shown in Fig. 8b. Here, we have significant increase of the thickness of the structure $h^{(\mathrm{opt})}/h^{(\mathrm{init})} = 13.56$ and large reduction of the elastic energy $U^{(\mathrm{init})}/U^{(\mathrm{opt})} = 151.45$.

5.2 Example: reinforcement of plate by ribs

The rectangular plate (3,000 mm × 2,000 mm) shown in Fig. 9a is analyzed (cf. Bojczuk and Szteleblak 2005). The structure is made of steel (Young's modulus is $E = 2.05 \cdot 10^5$ MPa and Poisson's ratio is $\nu = 0.3$). Its initial thickness is 15 mm. The plate is clamped on three edges, while the fourth (upper) edge is free. Transverse load varies linearly along the height of the plate.

Here, the optimization problem (68) corresponds to minimization of the strain energy of the structure with constraint imposed on the total volume of the plate, where C_0 corresponds to the initial volume. It is assumed that ribs connect points on the boundary of the structure. Also, geometrical constraints limiting minimum distance between non-intersecting ribs to 200 mm and the minimum thickness of the plate to 10 mm, are used.

Rectilinear ribs of cross-sectional dimensions: width $a_2 = 50$ mm, total height $h_2 = 40$ mm, are introduced into positions, which are specified from the solution of the problem of initial localization. It corresponds

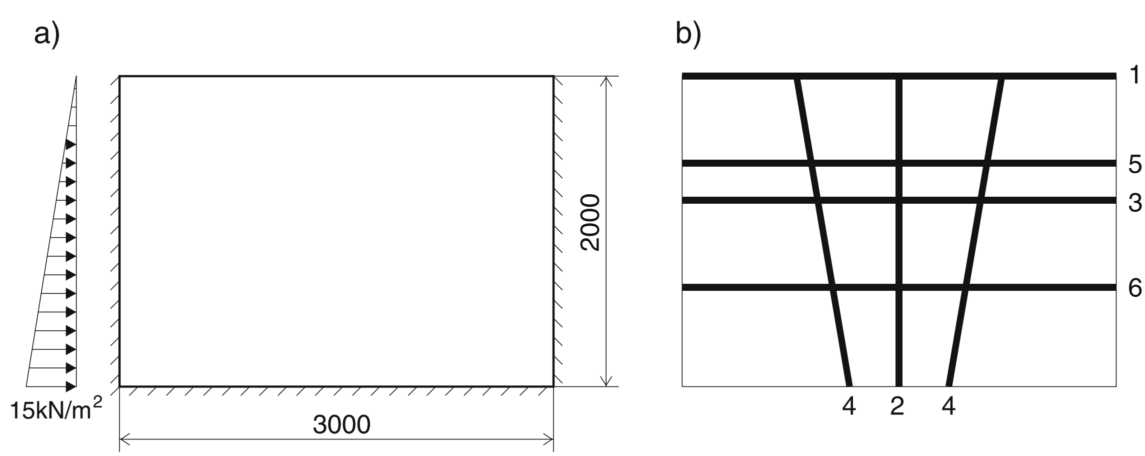

Fig. 9 Optimal design of plate under transverse load reinforced by ribs: **a** geometry of the plate; **b** optimal layout of ribs

to minimization of the topological derivative (77) of Lagrangian with respect to positions of the ribs ends. In the first stage, seven ribs are introduced, and next, slight correction of their position is performed. The constraint imposed on minimum thickness of the plate is active. Figure 9b shows layout of ribs and order of their introduction. The ratio of the strain energies of the initial design and optimal design is $G^{(\mathrm{init})}/G^{(\mathrm{opt})} = 2.35$.

6 Conclusions

The expressions for topological derivative with respect to introduction of small circular holes and with respect to introduction of stiffeners into plates are derived in the paper. Next, the heuristic algorithms of topological optimization of plates are formulated. In particular, the finite topology modification approach, which uses topological derivative with respect to introduction of holes, is applied in problems of topology and shape optimization of plates. Moreover, in problems of optimization of plates with reinforcement, topological derivative is used in order to determinate initial position of ribs.

Numerical examples shown in the paper confirm applicability and usefulness of the approach based on the topological derivative concept. It is noted, that the application of finite modifications essentially reduces computation time required for generation of improved or optimal designs.

References

Allaire G (2002) Shape optimization by the homogenization method. Springer, New York
Allaire G, Jouve F, Toader A-M (2002) A level set method for shape optimization. CR Acad Sci Paris, Série I 334: 1125–1130
Allaire G, Jouve F, Toader A-M (2004) Structural optimization using sensitivity analysis and a level set method. J Comp Phys 194:363–393
Allaire G, de Gournay F, Jouve F, Toader A-M (2005) Structural optimization using topological and shape sensitivity via a level set method. Control Cybern 34:59–80
Bendsoe MP (1997) Optimization of structural topology, shape and material. Springer, Berlin
Bendsoe MP, Kikuchi N (1988) Generating optimal topologies in structural design using a homogenization method. Comp Meth Appl Mech Eng 71:197–224
Bojczuk D (2006) Method of optimal reinforcement of structures based on topological derivative. In: Mota Soares C et al (eds) Proceedings of the III European conference on computational mechanics. Springer, Lisbon, on CD-ROM
Bojczuk D, Mróz Z (1998a) On optimal design of supports in beam and frame structures. Struct Optim 16:47–57
Bojczuk D, Mróz Z (1998b) Optimal design of trusses with account for topology variation. Mech Struct Mach 26:21–40
Bojczuk D, Mróz Z (1999) Optimal topology and configuration design of trusses with stress and buckling constraints. Struct Optim 17:25–35
Bojczuk D, Mróz Z (2005) Determination of optimal actuator forces and positions in smart structures using adjoint method. Struct Multidisc Optim 30:308–319
Bojczuk D, Szteleblak W (2005) Topology and shape optimization of plates using finite variations. In: Proceedings of the 16th international conference on computer methods in mechanics, Częstochowa (Poland), on CD-ROM
Bojczuk D, Szteleblak W (2006) Application of finite variations to topology and shape optimization of 2D structures. J Theoret Appl Mech 44:323–349
Bojczuk D, Szteleblak W (2008) Optimization of layout and shape of stiffeners in 2D structures. Comp Struct 86:1436–1446
Burczyński T, Kokot G (2003) Evolutionary algorithms and boundary element method in generalized shape optimization. J Theor Appl Mech 41:341–364
Burger M, Hackl B, Ring W (2004) Incorporating topological derivatives into level set method. J Comp Phys 194: 344–362
Cea J, Garreau S, Guillaume P, Masmoudi M (2000) The shape and topological optimizations connection. Comput Methods Appl Mech Eng 188:713–726
Dems K, Mróz Z (1984) Variational approach by means of adjoint systems to structural optimization and sensitivity analysis. II. Structure shape variation. Int J Solids Struct 19:527–552
Dems K, Mróz Z (1989) Shape sensitivity analysis and optimal design of physically nonlinear plates. Arch Mech 41(4): 481–501
Eschenauer HA, Kobelev VV, Schumacher A (1994) Bubble method for topology and shape optimization of structures. Struct Optim 8:42–51
Garreau S, Guillaume P, Masmoudi M (2001) The topological asymptotic for PDE systems: the elasticity case. SIAM J Control Optim 39:1756–1778
Kirsch U (1989) Optimal topologies of structures. Appl Mech Rev 42:223–239
Lewiński T, Telega JJ (2000) Plates, laminates and shells. Asymptotic analysis and homogenization. World Scientific, Singapore
Mróz Z, Bojczuk D (2000) Topological derivative and its application in optimal design of truss and beam structures for displacement, stress and buckling constraints. In: Rozvany GIN, Olhof N (eds) Topology optimization of structures and composite continua. Kluwer, Boston, MA, pp 91–105
Mróz Z, Bojczuk D (2003) Finite topology variation in optimal design of structures. Struct Multidisc Optim 25:153–173
Mróz Z, Bojczuk D (2006) Topological sensitivity derivative: application in optimal design and material science. Found Civ Envir Eng 7:229–250
Novotny AA, Feijóo RA, Padra C, Taroco E (2005) Topological derivative for linear elastic plate bending problems. Control Cybern 34:339–361
Osher S, Sethian JA (1988) Front propagating with curvature dependent speed: algorithms based on Hamilton–Jacobi formulations. J Comp Phys 78:12–49
Osher S, Santosa F (2001) Level set methods for optimization problems involving geometry and constraints: I. Frequencies of a two-density inhomogeneous drum. J Comp Phys 171:272–288
Petryk H, Mróz Z (1996) Time derivatives of integrals and functionals defined on varying volume and surface domains. Arch Mech 38:697–724

Sethian JA, Wiegmann A (2000) Structural boundary design via level set and immersed interface methods. J Comp Phys 163:489–528
Sokołowski J, Żochowski T (1999) On topological derivative in shape optimization. SIAM J Control Optim 37:1251–1272
Sokołowski J, Żochowski T (2003) Optimality conditions for simultaneous topology and shape optimization. SIAM J Control Optim 42:1198–1221
Timoshenko S, Woinowsky-Krieger S (1959) Theory of plates and shells. McGraw-Hill
Wang X, Wang MY, Guo D (2004) Structural shape and topology optimization in a level-set-based framework of region representation. Struct Multidisc Optim 27:1–19
Woźniak C (ed) (2001) Mechanics of elastic plates and shells [in Polish]. PWN, Warszawa
Xia Q, Wang MY, Wang S, Chen S (2006) Semi-Lagrange method for level-set based structural topology and shape optimization. Struct Multidisc Optim 31:419–429
Xie YM, Steven GP (1993) A simple evolutionary procedure for structural optimization. Comp Struct 49:885–896